

## P6R.2 THE FRONT RANGE PILOT PROJECT FOR GPM: AN INSTRUMENT AND CONCEPT TEST

S. A. Rutledge<sup>\*1</sup>, R. Cifelli<sup>1</sup>, T. Lang<sup>1</sup>, S. Nesbitt<sup>1</sup>, K. S. Gage<sup>2</sup>, C. R. Williams<sup>2,3</sup>, B. Martner<sup>2,3</sup>, S. Matrosov<sup>2,3</sup>, V. Bringi<sup>1</sup>, and P. C. Kennedy<sup>1</sup>

<sup>1</sup>Colorado State University, Fort Collins, CO

<sup>2</sup>NOAA Aeronomy Laboratory, Boulder, CO

<sup>3</sup>CERES, University of Colorado, Boulder, CO

### 1. INTRODUCTION

In the summer of 2004, demonstration of the supersite ground validation (GV) concept for the Global Precipitation Measurement (GPM) mission was carried out in the form of a Front Range Pilot project (FRP), involving scientists from CSU and NOAA's Environmental Technology Laboratory and Aeronomy Laboratory. The project's specific aims included evaluation of dual-wavelength polarimetric radar observations for estimating rainfall rates in moderate to heavy rainfall, as well as developing errors associated with these techniques by comparison to ground-based measurements from gauges and disdrometers. To accomplish this component, the project used the S-Band CSU-CHILL radar at Greeley, CO and NOAA-ETL's X-Band radar at Erie, CO. The X-Band radar's improved phase sensitivity in light rain was also used to explore how polarimetric based techniques could be extended to light rainfall regimes. The pilot project also focused on selection of UHF profiler frequencies that would best complement S-Band profiler measurements to allow for the most accurate retrieval of drop size distribution characteristics. A further goal of the pilot project was to perform quantitative comparisons of drop size distribution (DSD) characteristics between the profilers and scanning radars in order to evaluate assumptions in the scanning radar retrieval technique (e.g., equilibrium drop shape relationship) as well as spatial variability of the DSD. We also looked to demonstrate the complimentary role played by rain gauges and surface disdrometers (both 2-D video and J-W types) in determining the error characteristics of multi-frequency profiler DSD estimates and dual-frequency radar DSD and rain estimates.

### 2. EXPERIMENTAL DESIGN

A diverse set of instrumentation was available for the pilot project, as illustrated in Fig. 1. The CSU-CHILL National Radar Facility was operated at its home base in Greeley, CO (<http://www.chill.colostate.edu>). Both the BAO and Platteville sites used profilers operating at 3 frequencies: one at S-Band to measure precipitation velocity spectra, and two in the UHF band: 915 and 449 MHz to try to separate air motion from precipitation particle motion. The UHF profilers were evaluated to determine their ability: 1) to resolve both the clear air and precipitation components of the radial velocity spectra in different precipitation environments (e.g., light

vs. heavy rain); and 2) in concert with the S-Band profiler data, provide dual-wavelength DSD parameter retrievals with the best performance. Each site was instrumented with at least one J-W impact-type disdrometer, tipping-bucket rain gauge, and surface meteorological station. CSU's 2-D video disdrometer was deployed to the BAO site (after June 1 to June 22), and was deployed at PLT thereafter.

#### 2.1 Radar scanning

The NOAA X-Band radar scanning sequence included 2 low-level PPIs and 2 RHIs covering the Platteville and BAO sites. Gate to gate resolution was set to either 150 m or 112.5 meters, giving a maximum range of 38.8 or 28.8 km, respectively. The CSU-CHILL scan sequence included a sector of approximately 40 degrees azimuth over the entire X-Band scan sector (and the instrumented sites), and specific RHIs over the BAO and Platteville instrumented sites. CHILL used two scanning modes depending on the rainfall regime: (1) a high-resolution 75 m range resolution low level scan mode matching with a 2-3 minute scan repeat cycle (allowing high-resolution quick scanning of surface rainfall), and (2) a standard resolution 150 m range resolution volume scan mode with a 6-8 minute scan repeat cycle (allowing storms' vertical reflectivity and microphysical structure to be scanned by CHILL).

Combining the S- and X-Band radar polarimetric measurements will allow comparison of measurements of rain rate and DSD characteristics, and evaluation of errors in those fields from both instruments. By using CHILL's unattenuated reflectivity field, it is possible to evaluate the X-Band's self-correcting specific differential phase method of accounting for attenuation. In addition, the X-Band system's higher differential phase sensitivity in light rain allows the quantification of errors in rain estimates in light rain from the less phase-sensitive S-Band CHILL radar. In addition, the measurements from the scanning radars can be compared with the estimates of rain rate and DSD characteristics from the surface disdrometers, profilers, and rain gauges to determine their error characteristics.

### 3. PROJECT TIMELINE AND CASES

The formal period of data collection period for the Front Range Pilot Project was 15 May through 21 June 2004, with some data collection done on a "target of opportunity" basis continuing during the summer.

Table 1 shows a list of cases collected during the pilot. Weather conditions were relatively dry during the first half of the project. The second half of the project brought more favorable conditions with a number of

---

*\*Corresponding author address:* Prof. Steven A. Rutledge, Department of Atmospheric Science, Colorado State Univ., Fort Collins, CO 80523-1371. E-mail: [rutledge@atmos.colostate.edu](mailto:rutledge@atmos.colostate.edu)

Table 1: List of cases collected during the GPM Pilot Project from 15 May 2004 through 21 June 2004. Asterisk indicates priority cases.

A = Polarimetric radar estimates of rainfall rates and drop sizes compared with profilers, disdrometers, or rain gauges  
 B = Testing X-band attenuation corrections using CHILL as un-attenuated reference  
 C = Basic studies of severe storm structure, kinematics, etc.

Case	Description	A	B	C	Problems
15MAY	weak convective clouds with sprinkles		x		
17MAY	conv. sprinkles				
20-21MAY	supercell thunderstorm with hail and tornadoes	x (PLT)	x	x	
22-23MAY	rainbands, one became MCS with hail	x (PLT, BAO)	x	x	
24-25MAY *	numerous thunderstorm cells	x (PLT, BAO)	x		BAO disdrom down, CHILL scanning stopped
29MAY *	convective cells, stratiform BB rain	x (PLT)	x		
4JUNE	conv. cell near Broomfield and farther south	x (BRF gauge?, urban flood gauge network?)			
9JUNE	nocturnal thunderstorms, mostly along foothills	x (BAO)			CHILL not on late
9-10JUNE *	numerous showers	x (PLT, BRF)	x		X-band not on early
12JUNE	brief showers	x (BAO)	x		
14-15JUNE	small convective showers in sector	x (TCA gauge?)	x		BAO disdrom down late
16-17JUNE *	light rain, then stronger cells, good rain accumulations	x (BAO, PLT)	x		
17-18JUNE *	widespread rain, good rain accumulations	x (BAO, PLT)	x		CHILL down late
18-19JUNE *	stratiform rain, good rain accumulations	x (BAO, PLT)	x		CHILL not on early
19-20JUNE *	showers in sector, some time series	x (BAO, PLT)	x		short outages at x-band
21JUNE *	line of moderate rain followed by light widespread rain	x (BAO, PLT, BRF)	x		X-band not on early

continuous light and heavy rain events (and at least one significant hailstorm) being observed. The heavy rain events are useful for comparing the S-band unattenuated rain estimates against the X-band attenuation corrected rain estimates. The X-band reflectivity and differential reflectivity fields are corrected for attenuation using the differential phase ( $\phi_{dp}$ ) field.

Additional cases (not shown in Table 1) included scattered light rain showers on 30 June, showers along with a bright band event on 15-16 July, widespread rain with embedded cells and occasional heavy rain on 22-23 July, and widespread rain with strong embedded convection on 23-24 July 2004. All in all favorable weather conditions occurred in the pilot, even though Colorado was still in a period of drought.

#### 4. RESULTS

In this section we concentrate on showing examples of data collected by the various platforms.

##### 3.1 S- and X- Band Radar Comparisons

The FRPP used comparisons of S- and X-Band polarimetric rainfall and DSD retrievals to show the following for GPM-GV:

- X-Band radar is capable of detecting useable  $K_{dp}$  magnitudes in rain rates as low as  $\sim 2 \text{ mm hr}^{-1}$ ; useable S-Band  $K_{dp}$  data cannot be obtained at rain rates of approximately  $5\text{-}7 \text{ mm hr}^{-1}$ . X-Band  $K_{dp}$  estimators are thus able to perform over a significantly larger portion of raining area and extend polarimetric rain estimation capabilities lower into the rain rate distribution than those at S-Band (Fig. 3), which allow improvement in rain estimates in this rain rate estimates over traditional Z-R techniques (Fig 4).
- Under high rain rate conditions (rates of several tens of  $\text{mm hr}^{-1}$ ) X-Band signals are subject to severe attenuation losses. While X-Band attenuation-correction procedures have been developed, complete signal extinction can occur along ray paths containing heavy rain and/or hail. Uncertainty in X-Band  $Z_{dr}$  corrections in attenuated conditions need further evaluation (Fig. 5).
- Both S- and X-Band multiparameter radar measurements ( $Z$ ,  $Z_{dr}$ ,  $K_{dp}$ ) may be used to estimate parameters of the rain DSD, such as parameters of the gamma DSD ( $D_m$ ,  $N_w$ ).
- Hydrometeor Identification may be employed reliably at both S- and X-Band in order to identify appropriate hydrometeor types within the radar scanning volume (apart from regions of complete attenuation at X-Band) (Fig. 6)

#### 5. PROFILERS IN THE SUPERSITE CONCEPT

Multi-frequency profilers will play several crucial roles within the Supersite:

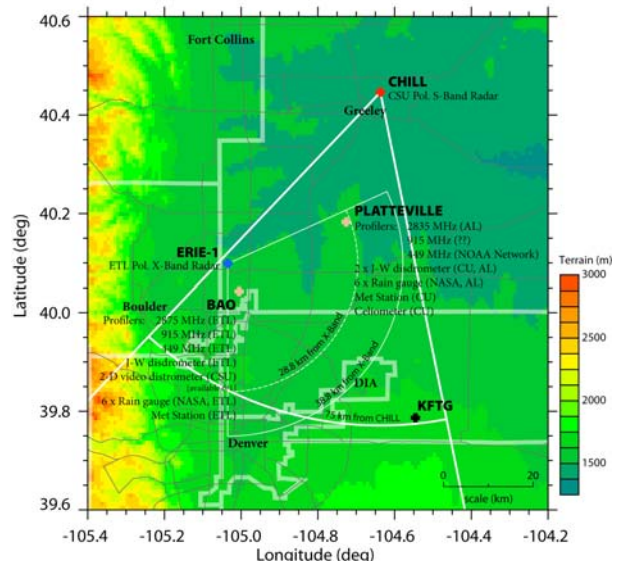


Fig. 1. Arrangement of observational platforms along the Front Range of Colorado used in the GPM Pilot Project.

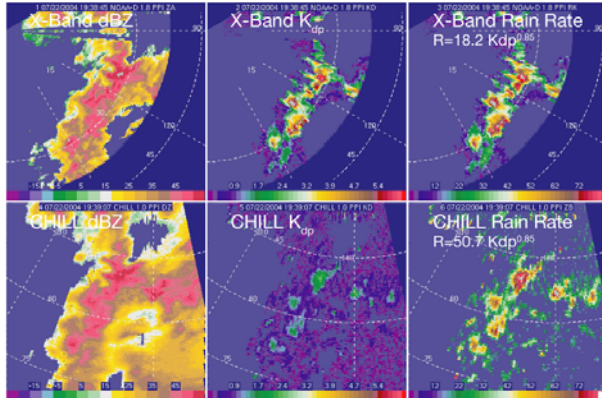


Fig. 3: 22 July 2004, ~1938 UTC PPI sector scans from X-Band (top row) and CHILL (bottom row) showing radar reflectivity (dBZ, left column),  $K_{dp}$  ( $\text{deg km}^{-1}$ , center column), and rain rate from the  $K_{dp}$  estimator ( $\text{mm hr}^{-1}$ , right column).

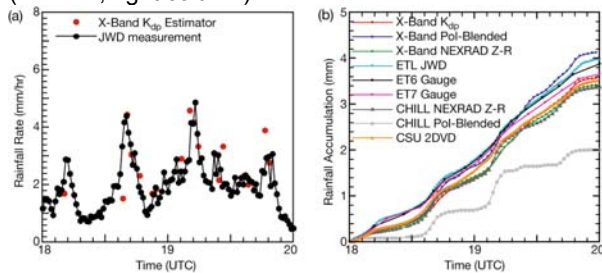


Fig. 4: For 21 June 2004: (a) rainfall rates from JWD and X-band  $K_{dp}$ -based estimators, (b) rainfall accumulations from different radar estimators and ground-based instruments. Rain rates were too light for useful S-Band polarimetric rain retrievals in this case.

- Measure reflectivity and estimate DSD parameters with very high vertical resolution down to heights very close to the surface (Fig. 7),
- Examine hydrometeor types and fall speeds with height through examination of multi-frequency Doppler spectra (Fig. 8),
- Used with surface disdrometers and rain gauges, profilers can link ground-based in situ measurements with scanning radar measurements at altitude,
- Provide independent, high temporal (1 min) and spatial (25 m) resolution measurements of rainfall and DSD variability to assess measurement, parameterization, and representativeness error of the scanning radar measurements.

Results from the FRPP showed that a S-Band- 449 MHz profiler pair will best provide information to retrieve DSD parameters at the Supersite due to the 449 MHz profiler's better ability to retrieve air motion (through Bragg scattering) relative to a 915 MHz profiler such that drop fall speeds may be separated from draft structures.

## 6. MULTI-INSTRUMENT SYNTHESSES

### 6.1 15-16 July 2004 Case: Comparisons from PLT

The 15-16 July 2004 case brought two differing storm cells to the Platteville Atmospheric Observatory in terms of their vertical structure and rainfall intensity. Fig. 9, panel (a) shows a time-height plot of S-Band reflectivity measured by the NOAA-AL profiler for the time period encompassing the two cells of interest. A newly developed convective cell passed directly over the ground site, beginning around 2230 UTC 15 July (Julian Day 197.94). Note reflectivities above 40 dBZ above the melting level (4.5 km MSL in this case), indicating the presence of convective precipitation in the first portion of this cell. Also note the tilt of the reflectivity profiles in the lowest 1 km AGL likely due to the advection of precipitation particles by the ambient wind. The second precipitation event was longer lasting and had stratiform rain characteristics as indicated by

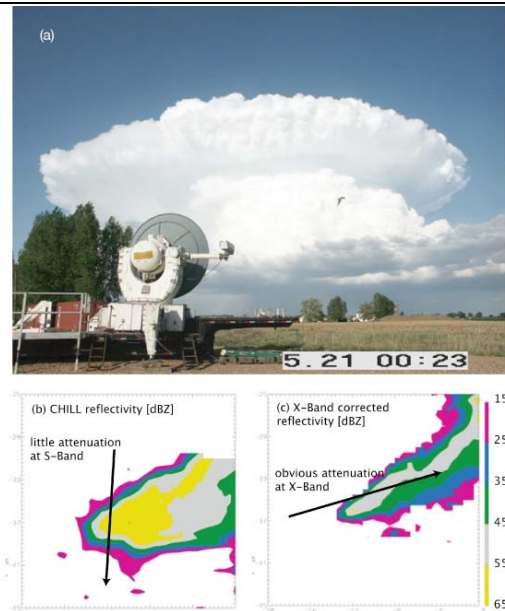


Fig. 5: (a) Photograph of X-Band radar scanning a supercell to the northeast near PLT at 00:23 UTC 21 May 2004. At 0023 UTC: (b) CHILL (S-Band) "unattenuated" reflectivity (dBZ) and (c) X-Band attenuation-corrected reflectivity (dBZ). The arrows indicate approximate beam propagation paths.

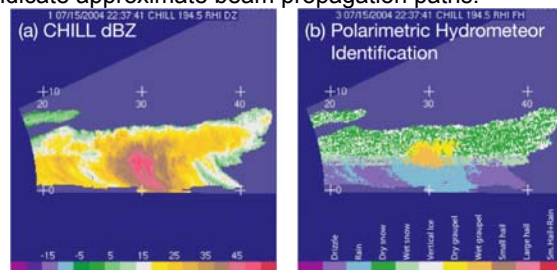


Fig 6: CHILL reflectivity RHI (a) and hydrometeor identification (b) from 22:37 UTC 15 July 2004.



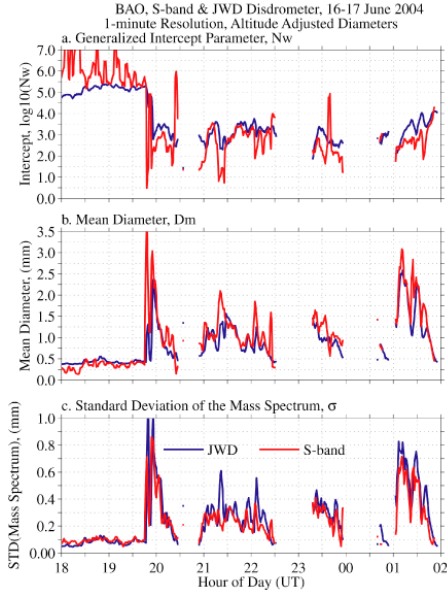


Fig. 7: Rain drop size parameters estimated from the JWD (blue) and S-band profiler at 316 m above the ground (red). Panel (a) shows the Generalized Intercept Parameter,  $N_w$ , Panel (b) shows mean drop diameter,  $D_m$  and Panel (c) shows the standard deviation of the Mass spectrum,  $\sigma$ .

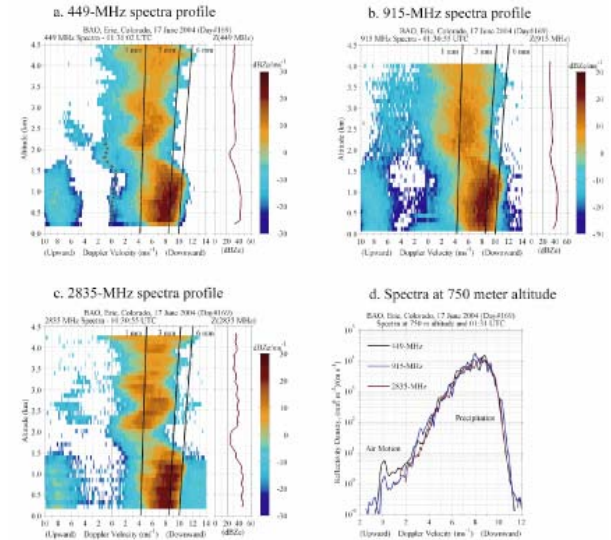


Fig. 8: Simultaneous spectra obtained from the three different frequency profilers at BAO. Panels (a), (b), and (c) shows the vertical profile of spectra collected from the 449 MHz, 915 MHz, and 2835 MHz profilers. Panel (d) shows the spectra for each profiler at the altitude of 750 meters above the ground. The air motion (Bragg scattering) portion of the spectrum occurs around  $0 \text{ m s}^{-1}$ , and the raindrop motion (Rayleigh scattering) portion of the spectrum occurs at more downward velocities.

the presence of a radar bright band throughout most of the event.

Fig. 9, panel (b) shows a time-height plot of S-Band/449 MHz retrieval of mass-weighted mean diameter  $D_m$ , retrieved using a technique similar to Schafer et al. (2002) described in section 3. Note that the time axes are identical in the two plots; however, the height scale has been expanded in panel (b) to examine the rain region in detail. In the first convective cell, there exist high mass-weighted particle sizes (many regions exceeding 2.5 mm) within the high-reflectivity convective region. Within the more stratiform event later on, modal  $D_m$  values range within smaller values, between 1 to 2 mm.

To compare both surface based and scanning radar estimates of  $D_m$ , Fig. 10 shows time series of (a) profiler and polarimetric radar estimated- and (b) profiler and altitude-corrected surface disdrometer estimated- $D_m$  for the time period shown in Fig. 9. For the radar-profiler comparison in panel (a), profiler  $D_m$  estimates were averaged over the vertical extent of the half-power beamwidth of the main lobe of the CHILL 1.5° and X-Band 1.8° beams, respectively. The height ranges of the scanning radar beams used to vertically average the profiler data are indicated by the white boxes in panel (b) of Fig. 9. Mass-weighted mean diameter is calculated from the radar measured differential reflectivity  $Z_{dr}$  using the following equations:

$$D_m = 1.619Z_{dr}^{0.485} \text{ at S-Band, and}$$

$$D_m = 1.6Z_{dr}^{0.49} \text{ at X-Band.}$$

From the time series in Fig. 10a, it is apparent that the profiler sees overall higher peak  $D_m$  values within the convective cell than either radar. The X-Band estimates higher  $D_m$  than CHILL for this cell, and the X-Band  $D_m$  values are overall in better agreement with the profilers

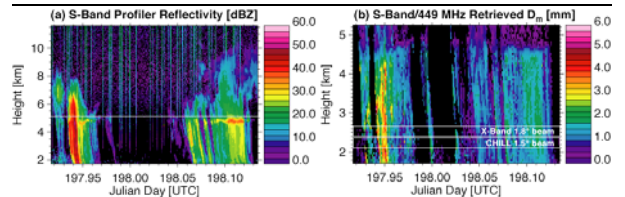


Fig. 9: For 15-16 July 2004: (a) Time series of the vertical profile of measured equivalent reflectivity [dBZe] from the NOAA-AL S-Band profiler. (b) Time-series of the vertical profile of S-Band/449 MHz retrieved mass-weighted mean diameter  $D_m$ . The sample volume of the scanning radars is denoted by the white rectangles.

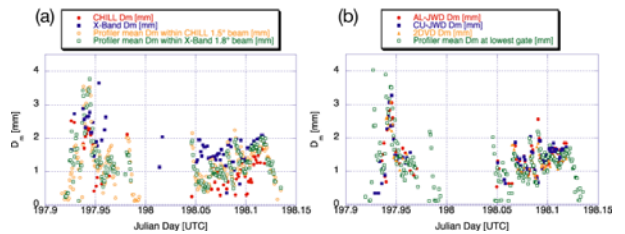


Fig. 10: (a) Time series of  $D_m$  estimates from the polarimetric scanning radars and average profiler-retrieved values within the scanning radars' sample volume. (b) Time series of  $D_m$  estimates from the surface disdrometers and profiler-retrieved values at 186 m  $\Delta Z$

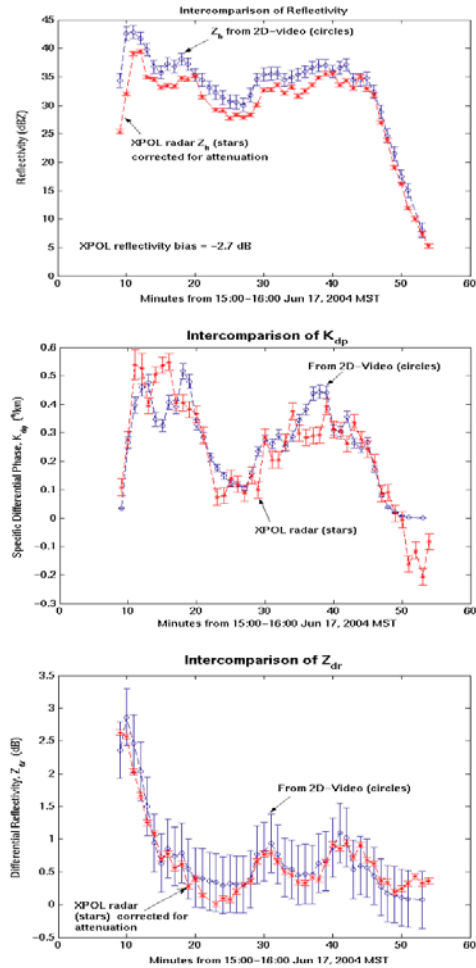


Fig. 11: Intercomparison of  $Z$  (top),  $K_{dp}$  (middle) and  $Z_{dr}$  (bottom) from X-Band radar and 1 min averaged 2DVD measurements of DSD. Standard deviation bars for 2DVD data are based on expected sampling errors, while those from radar are based on expected signal fluctuation errors. Radar data averaged over a 700 m<sup>2</sup> area centered on the 2DVD location.

during this first cell than CHILL. In the later stratiform precipitation, again the X-Band  $D_m$  values are higher than CHILL's, however CHILL's values seem in better agreement with the profiler measurements made at its scan elevation than for X-Band.

Fig. 10b shows a  $D_m$  profiler-surface disdrometer time series comparison for these two cells. Profiler  $D_m$  retrievals are taken from the lowest bin in the data, at 186 m AGL, while the AL- and CU-Joss-Waldvogel Disdrometers (AL-JWD and CU-JWD) and the CSU 2DVD are collocated at the surface. Good agreement overall is present between the profilers given the sample volume differences between the profiler and the disdrometer, with the profiler retrievals having somewhat more temporal variability.

## 5.2 Disdrometer-radar comparisons

The 2DVD gamma DSD can also be used to simulate the radar observables such as  $Z$ ,  $Z_{dr}$  and  $K_{dp}$  and these can be compared with the corresponding radar measurements made by the NOAA/X-Band radar as illustrated in Fig. 11. The standard error bars for the 2DVD data are based on expected sampling errors (sensing area= 100 cm<sup>2</sup>, time integration=1 min) while those for the radar are based on expected fluctuation errors. The radar data have been averaged over a 700 × 700 m area centered over the location of the 2DVD. The bias in  $Z$  was determined to be -2.7 dB. The bias in  $Z_{dr}$  was determined to be very small (<0.1 dB). Note in Fig. 11b that the minimum detectable  $K_{dp}$  at X-band is close to 0.1 deg/km or around 2 mm/h. This figure demonstrates the advantage of X-band for measuring low rain rates. At higher rain rates, the X-band signal generally falls below noise level while this is not a problem at S-band. Thus, to optimally cover the full range of rain rates with polarimetric methods, a combined S/X-band radar system with dual-polarization at both frequencies is desired. Below 2 mm/h however, the standard Z-R method can be used. Having a network of 2DVD disdrometers (rather than the usual rain gages) will enable the radar  $Z$  and  $Z_{dr}$  data to be very accurately calibrated. At the same time it will enable the development and validation of DSD retrieval algorithms based on dual-frequency radar measurements of  $Z$ ,  $Z_{dr}$  and  $K_{dp}$ . The full power of dually-polarized radar techniques for rain measurement will be significantly enhanced by deploying a network of 2DVDs within the scanning range of a dual-frequency radar system.

## 7. SUMMARY

The FRPP has marked the beginning of trade studies defining the location and instrumentation of the GPM-GV midlatitude Supersite. To accomplish the GV task, instrumentation recommendations from the FRPP collaborators for the Supersite include:

- Dual wavelength (S- and X- band) scanning dual-polarization Doppler radar
- Dual wavelength (S-Band and 449 MHz) vertically pointing profiler system
- Network of surface disdrometers, mix of 2DVD and J-W types based on cost, utility
- Extensive network of tipping bucket rain gauges

For more information visit:

<http://radarmet.atmos.colostate.edu/gpm>

## 8. ACKNOWLEDGEMENTS

We thank all who participated in the Pilot Project including staff from the CSU-CHILL Facility (Pat Kennedy, Dave Brunkow and Bob Bowie), CSU's Engineering Dept. (Miguel Gavez), and NOAA's Aeronomy Lab and Environmental Technology Lab. Funding for the FRPP was provided by NASA under the direction of Ramesh Kakar and Richard Lawrence. Post-project analysis funding has been provided by NASA under Matthew Schwaller. The CSU-CHILL

National Radar Facility is operated by the National Science Foundation.